Available online at www.sciencedirect.com
SCIENCE DIRECT®
Thermochimica Acta 413 (2004) 127–137
thermochimica acta
www.elsevier.com/locate/tca

Thermodynamic optimization of the In–Pb–Sn system based on new evaluations of the binary borders In–Pb and In–Sn

N. David [a], Khadija El Aissaoui [b], J.M. Fiorani [a,*], J. Hertz [a], M. Vilasi [a]

[a] *Laboratoire de Chimie du Solide Minéral, UMR 7555, Université Henri Poincaré Nancy-I, F–54506 Vandœuvre-Lès-Nancy, France*
[b] *Laboratoire de Thermodynamique Métallurgique et Rhéologie des Matériaux, Université Ibnou Zohr, 80000 Agadir, Morocco*

Received 28 April 2003; received in revised form 13 October 2003; accepted 28 October 2003

Abstract

A new assessment of two binary In–Pb and In–Sn systems and a thermodynamic description of the ternary In–Pb–Sn system are presented in this paper. The modeling of each system is carried out in the same way, by taking into consideration available thermodynamic and phase diagram data. The thermodynamic description of pure elements is taken from the Scientific Group Thermodata Europe (SGTE) data bank [Calphad 15 (1991) 317]. The lattice stability of In, Pb and Sn in the γ-phase, which is not available, is evaluated. The liquid phase, the three primary solid solutions (In), (Pb) and (βSn), and the two intermediate phases β and γ, are described by Redlich–Kister–Muggianu formalism as disordered solutions. The thermodynamic description is performed according to the Calphad method [Computer Calculation of Phase Diagrams, Academic Press, New York (1970)] by using the Thermo-Calc software [Calphad 9 (1985) 153] and the Parrot program [Ph. D. Thesis, Royal Institute of Technology, Stockholm (1984)]. The adjustable parameters obtained and the calculated phase diagrams are presented. For the two binary systems and the ternary system, some calculated thermodynamic functions are compared with experimental values of liquid alloys as well as of solid alloys.

Keywords: In–Pb; In–Sn; In–Pb–Sn; Thermodynamic modeling; Calphad method

1. Introduction

Being interested in the miscibility gap of the liquid phase in the multicomponent system Cu–In–Pb–Sn–Zn, we developed an accurate data bank which can be used by the Thermo-Calc program [3] to evaluate the existence of this miscibility gap by using a multicomponent phase diagram calculation. The base of this data bank was the modelisation of the 10 binary subsystems and, as far as possible, of the 10 ternary subsystems. All these optimizations are performed according to the Calphad method [2] in the Redlich–Kister–Muggianu formalism [5,6]. We performed a new description of the In–Sn system because Vassiliev et al. [7] published an exploration of the liquid phase by electromotive force measurements on the whole system which is more recent than the last assessments due to Lee et al. [8] and Korhonen and Kivilahti [9] (both are based on the earlier electromotive force measurements of Terpilowski and Przezdziecka-Mycielska [10]). We also optimized the In–Pb system, because for this binary border, to our knowledge, there does not exist some optimization based on the thermodynamic descriptions taken from the Scientific Group Thermodata Europe (SGTE) data bank collected by Dinsdale [1]. For the description of the third binary border, Pb–Sn, we have opted to the optimized set of parameters determined by Ohtani et al. [11].

The ternary In–Pb–Sn description is based on the enthalpy of mixing measurements by Fiorani et al. [12] and on thermal analysis data obtained by Evans and Prince [13]. We have used the Parrot program [4] to determine the adjustable parameters of the thermodynamic description and compared them to data available in literature.

2. Review of experimental data

2.1. In–Pb

The In–Pb phase diagram is determined by two peritectic reactions whose invariant temperatures are located

* Corresponding author. Tel.: +33-3-83-68-46-51; fax: +33-3-83-68-46-50.
E-mail address: fiorani@lcsm.uhp-nancy.fr (J.M. Fiorani).

0040-6031/$ – see front matter © 2003 Elsevier B.V. All rights reserved.
doi:10.1016/j.tca.2003.10.020

between the melting points of the two elements. An intermediate β-phase separates the two primary solid solutions. The liquidus was studied first by Kurnakow and Puschin [14] over the entire composition range. Valentiner and Haberstroh [15] have done a reinvestigation by thermal analysis and have indicated the existence of the two peritectic equilibria: Liquid + (Pb) → β at 445.05 K and Liquid + β → (In) at 432.35 K.

Hansen and Anderko [16] have given an assessed In–Pb phase diagram based on experimental works of many authors. Hultgren et al. [17] compiled thermodynamic data from papers before 1973. Recently a critical assessment of the binary system was made by Nabot and Ansara [18]. They have also proposed a thermodynamic description of the system and given the thermodynamic properties of the different phases expressed with the Redlich–Kister formalism [5]. Kao [19] has published another calculated phase diagram of the system using the Calphad approach. The Gibbs energy of the solution phases are modeled using the same expression as Ansara and Nabot. The two calculations are based on the same experimental data, thermodynamic values and phase diagrams. We have rejected the description of Ansara and Nabot because since 1987 (the date of their publication), the description of the lattice stability of (In) and (Pb) has changed and does not correspond to the data collected by Dinsdale [1]. Other works on this system was performed by Bolcavage et al. [20], by Kao [19], by Boa and Ansara [21] and by Zivkovic et al. [22]. Nevertheless, any of these good optimizations is based both on the thermodynamic descriptions of the pure elements and on the lattice stability parameters, taken from the Scientific Group Thermodata Europe (SGTE) data bank [1]. That is the reason why we preferred to reoptimize this binary system.

Table 1 gives experimental equilibria according to Massalski [23]. We only present the experimental data used for the modelisation and which are summarized in Table 2. For further detail the reader is referred to [18].

The liquidus, the solidus and the phase boundaries were determined by Kurnakow and Puschin [14], Ageew and Ageewa [24], Valentiner and Haberstroh [15], Klemm and Volk [25], Campbell et al. [26], Heumann and Predel [27], Liao et al. [28], Marcotte [29] and Evans and Prince [30].

The chemical potential of lead and its activity in liquid phase have been determined by different methods.

- A variety of vapor pressure techniques by Shiu and Munir (at 1000 and 1200 K) [31] and Sommer et al. (at 1000 K) [32].
- EMF method by Terpilowski and Gregorczyk (663–873 K) [33], Kameda et al. (859–1330 K) [34], Zheng and Kozuka (1023–1273 K) [35].
- Calorimetric investigations by Minic et al. [36].

The enthalpy of mixing in the liquid has been measured by calorimetric method by Scheil and Lukas (at 613 K) [37], Wittig and Scheidt (at 644 K) [38], and Naguet et al. (at 756 K) [39]. Heumann and Predel [27] measured the enthalpy of solidification of In–Pb alloys by quantitative thermal analysis. Yoon [40] measured the enthalpy of formation of solid alloys at 315 K in the range of composition x_{Pb} = 0.1 to 0.9.

2.2. In–Sn

This system has been explored many times. The temperature and the composition of the different equilibria were discussed a long time as well as the liquidus, the solidus curves and the stability range of the two intermediate phases whose boundaries differ according to the authors. Hansen and Anderko [16] have given an assessed In–Sn phase diagram based on experimental works of various authors. Hultgren et al. [17] proposed another compilation of papers published before 1973. The phase diagram that is now accepted is primarily based on the work of Heumann and Alpaut [41] who used several methods, differential thermal analysis (DTA), X-ray, dilatometric measurements and microscopic observations and on the work of Cakir and Alpaut [42]. The main difference between the phase diagram of Hansen and Anderko and those of Heumann and Alpaut is found in the stability region of the two intermetallics β(In-rich) and γ(Sn-rich).

The In–Sn phase diagram is formed by two peritectic reactions located near the pure elements and one eutectic reaction situated in the middle of the phase diagram. The system contains two intermediate phases with large ranges of solubility: a hexagonal Sn-rich γ-phase and a tetragonal In-rich β-phase which has the same space group as (In) but with a smaller c/a ratio. The eutectic equilibrium is formed by liquid and the two intermediate phases. The composition of the eutectic point is 48.3 at.% Sn and the eutectic temperature

Table 1
Calculated and assessed [23] temperatures and compositions of invariant reactions in the In–Pb system

Reaction	Assessed [23]				Calculated				Reaction type
	Compositions of the respective phases			Temperature (K)	Compositions of the respective phases			Temperature (K)	
Liquid+ β ⇔ (In)	10.16	12.67	11.56	432	10.2	13.9	10.5	432	Peritectic
Liquid+ (Pb) ⇔ β	19.5	29	26	445	19.8	28.7	25.7	445	Peritectic
Liquid ⇔ (In)	–	2.5	–	429	Not restituted				Congruent

The compositions are given in atomic% of lead.

Table 2
Summary of the experimental data used for the thermodynamic description of the In–Pb system

Reference	Experimental method	Data used
[14]	Thermal analysis	Liquidus temperatures
[15]	Thermal analysis, XRD	Phase boundaries, peritectic temperatures
[24]	Thermal analysis, XRD	Liquidus temperatures
[25]	Thermal analysis	Liquidus, solidus temperatures
[26]	XRD	Liquidus temperatures
[27]	Quantitative thermal analysis, XRD, resistivity measurements	Enthalpy of solidification Liquidus, solidus temperatures Congruent point
[28]	DTA	Liquidus, solidus temperatures
[29]	DTA	Liquidus, solidus temperatures
[30]	DTA	Liquidus, solidus, peritectic temperatures
[31]	Vapor pressure	Activity of Pb 663–873 K
[32]	Knudsen effusion method	Partial pressure of Pb at 1000 K
[33]	EMF	Activity of Pb 663–873 K
[36]	Calorimetry	Activity of Pb at 673, 773, 873 and 973 K
[37]	Calorimetry	Enthalpy of mixing at 613 K
[38]	Calorimetry	Enthalpy of mixing at 644 K
[39]	Calorimetry	Enthalpy of mixing at 756 K

is 393 K. The two peritectic reactions are formed by the liquid, one primary solid solution and an intermediate phase. The composition and the temperature of these reactions according to Massalski [23] are given on Table 3.

Recently the binary system was assessed by Lee et al. [8] and by Korhonen and Kivilahti [9]. The two modelisations were done by the Calphad method [2], using the Thermo-Calc software [3] and the Parrot program [4].

Korhonen and Kivilahti have done a new modelisation because the description of the lattice stability of (In) in the β-phase used by Lee et al. does not correspond to the data collected by Dinsdale [1]. This parameter is not the same in the primary (In) solid solution and in the (βIn) phases and this fact was taken into account in the paper of Lee et al. [8]. This difference is not really important for the calculation but the presence of this supplementary term is more correct and closer to physical reality. In the calculation of Korhonen and Kivilahti the In-rich boundary is displaced to higher In contents due to a different choice of experimental data set for this region used in the calculation. These choice origins from results obtained from calculations of the ternary Sn–In–Ag system.

In this paper we only present the experimental data used for the thermodynamic description in Table 4. Further details are found in the previous assessment of Hansen and Anderko [16], Hultgren et al. [17], Lee et al. [8] and Korhonen and Kivilahti [9].

The liquidus was determined first by Heumann and Alpaut [41] in the entire composition range. They used several experimental techniques and found three invariant reactions—two peritectic equilibria: Liquid + (In) → β at 416.15 K, Liquid + (βSn) → γ at 497.15 K and one eutectic equilibrium: Liquid → β + γ at 393.15 K. They have observed a kink in the γ-phase in the Sn-rich region. After the work of Heumann and Alpaut [41], the liquidus, the solidus and the phase boundaries have been determined by Predel and Gödecke [43] who used DTA in the Sn-rich region, by Evans and Prince [44] who used DTA and tensile testing in the whole composition range, and by Kaplun [45] who used vibration method and thermal analysis in the range 0–60 at.% Sn. Solid phase boundaries are determined by Wojtaszek and Kuzyk, using the measurements of the ratio of resistance in the range 60–100 at.% Sn [46]. We note that these authors have used the same method in the range 0–60 at.% Sn [47]. These results have not been taking into account in the calculation because the authors have suggested that the equilibrium of the concerning alloys was not good. Predel and Gödecke and Evans and Prince agree with the data of Heumann and Alpaut but did not observe the kink in the γ-phase.

Table 3
Calculated and assessed [23] temperatures and compositions of invariant reactions in the In–Sn system

Reaction	Assessed [23]				Calculated				Reaction type
	Compositions of the respective phases			Temperature (K)	Compositions of the respective phases			Temperature (K)	
Liquid+ β ⇔ (In)	10	14	12	416	10	13.1	12.9	415	Peritectic
Liquid ⇔ β + γ	48.3	44	77	393	48.1	43	77	393	Eutectic
Liquid + (βSn) ⇔ γ	95.7	99.5	99	497	96.3	98.9	98	497	Peritectic

The compositions are given in atomic% of tin.]

Table 4
Summary of the experimental data used for the thermodynamic description of the In–Sn system

Reference	Experimental method	Data used
[7]	EMF	Activity of In 630–830 K
[38]	Calorimetry	Enthalpy of mixing at 644 K
[41]	DTA, dilatometric measurements, XRD, microscopic observations	Liquidus, solidus temperatures Phase boundaries
[42]	EMF	Activity of In 348–393 K
[43]	DTA	Liquidus, solidus temperatures
[44]	DTA, tensile testing	Liquidus, solidus temperatures
[45]	Thermal analysis, vibration method	Liquidus, solidus temperatures
[46]	Ratio of resistance measurements	Solvus 60–100 at.% Sn
[47]	Ratio of resistance measurements	Solvus 0–60 at.% Sn
[48]	Calorimetry	Enthalpy of mixing at 723 K
[49]	Calorimetry	Enthalpy of mixing at 521 K
[50]	Calorimetry	Enthalpy of mixing at 723 K
[51]	Quantitative thermal analysis	Enthalpy of solidification

The chemical potential of indium and its activity in the liquid phase have been determined by EMF method by Terpilowski and Przezdziecka-Mycielska (673–873 K) for $x_{Sn} = 0.10–0.95$ [10] and Vassiliev et al. (630–830 K) for $x_{Sn} = 0.20–0.95$ [7]. The latter values are very accurate and reliable and do not correspond to the values obtained by Terpilowski and Przezdziecka-Mycielska especially in the In-rich side.

The enthalpy of mixing of the liquid has been measured by calorimetry in liquid tin solution by Kleppa (at 723 K) for $x_{Sn} = 0.66–0.94$ [48]. The direct calorimetric method was used by Wittig and Scheidt (at 644 K) for $x_{Sn} = 0.11–0.90$ [38], by Bros and Laffitte (at 521 K) over the entire composition range [49], and by Yazawa et al. (723 K) for $x_{Sn} = 0.10–0.95$ [50]. The discrepancy between the data of the various authors is low.

Concerning the solid phases, Alpaut and Heumann [51] measured the enthalpy of formation in In–Sn alloys by quantitative thermal analysis and Cakir and Alpaut have investigated the thermodynamic properties of solids by determination of the activity of indium by EMF measurements between 348 and 398 K [42].

2.3. In–Pb–Sn

There is only few experimental information available in literature concerning the phase diagram or the thermodynamic data. The liquidus and the solidus curves and the phase boundaries were determined by Campbell et al. [26] who studied 40 alloys, 13 of which contained less than 40 wt.% Sn. They found that no ternary eutectic occurs in the system, and that the β-phase in the binary In–Pb forms a continuous series of solid solutions with the β-phase in the binary In–Sn. Marcotte [29] using DTA measurements has investigated liquidus and solidus temperatures of 20 alloys the majority of which contained less than 30 wt.% Sn. These results are in agreement with the data of Campbell et al. [26]. Evans and Prince [13] have explored the ternary system in the composition range up to 25 wt.% Sn using thermal analysis. The compositions of the alloys are situated along sections at 30, 40 and 70 wt.% Sn, 2 and 25 wt.% In and the section joining the In–Sn binary and the Pb–Sn binary near the two eutectic points. In this article, they presented only graphics of the two sections at 2 wt.% In and the section between In–Sn eutectic and Pb–Sn eutectic. They reported two ternary invariant reactions: Liquid + (Sn) → (Pb) + γ at 444 K and Liquid + (Pb) → β + γ at 409 K.

Table 5
Summary of the experimental data used for the thermodynamic description of the In–Pb–Sn system

Reference	Experimental method	Data used
[12]	Calorimetry	Enthalpy of mixing at 717 K
[13]	Thermal analysis	Liquidus temperatures, phase boundaries Invariant temperature reactions
[26]	Thermal analysis, XRD, microscopic observations	Liquidus temperatures
[29]	DTA measurements	Liquidus temperatures

Skoropanov and Voronova [52] have proposed the integral mixing isoenthalpic curves from measurements in the ternary system. Fiorani et al. [12] have investigated the system by the drop method in a Calvet type calorimeter. The enthalpy of mixing measurements were performed following the three isoplethic section $x_{In} = x_{Pb}$, $x_{Sn} = x_{Pb}$ and $x_{In} = x_{Sn}$ at 717 K.

The set of data used in this modeling of the ternary system is summarized in Table 5.

3. Thermodynamic models

Six phases are meeting in the ternary system: liquid, (In), β, (Pb), γ and (βSn). The thermodynamic description is based on the data of pure elements taken from Scientific Group Thermodata Europe (SGTE) data bank [1] and from [8] for some lattice stability parameters. They are expressed

Table 6
Description of the Gibbs energy for the unary phases

Element	Phase	T (K)	${}^0G_i^{\varphi}(T) - {}^0H_i^{\Phi}$ (298.15 K) (J mol^{-1} of atoms)
In	(Pb)	298.14–3800	$+123 - 0.1988\ T + \text{GHSERIN}$
	(Sn)	298.14–3800	$2092 + \text{GHSERIN}$[a]
	(In)	298.14–429.76	$-6978.89 + 92.338115\ T - 21.8386\ T \ln T - 0.00572566\ T^2 - 2.120321 \times 10^{-06}\ T^3 - 22906\ T^{-1}$
		429.76–3800	$-7033.47 + 124.476492\ T - 27.4562\ T \ln T + 5.4607 \times 10^{-04}\ T^2 - 8.367 \times 10^{-08}\ T^3 - 211708\ T^{-1} + 3.30026 \times 10^{+22}\ T^{-9}$
	β	298.14–3800	$+193 - 0.16479\ T + \text{GHSERIN}$
	L	298.14–429.76	$+3282.152 - 7.63649\ T - 5.21918 \times 10^{-20}\ T^7 + \text{GHSERIN}$
		429.76–3800	$+3283.66 - 7.640174\ T - 3.30026 \times 10^{22}\ T^{-9} + \text{GHSERIN}$
Pb	(Pb)	298.14–600.63	$-7650.085 + 101.715188\ T - 24.5242231\ T \ln T - 0.00365895\ T^2 - 2.4395 \times 10^{-07}\ T^3$
		600.63–1200	$-10531.115 + 154.258155\ T - 32.4913959\ T \ln T + 0.00154613\ T^2 + 8.05644 \times 10^{25}\ T^{-9}$
		1200–3000	$+4157.596 + 53.154045\ T - 18.9640637\ T \ln T - 0.002882943\ T^2 + 9.8144 \times 10^{-08}\ T^3 - 2696755\ T^{-1} + 8.05644 \times 10^{25}\ T^{-9}$
	(Sn)	298.14–2100	$+489 + 3.52\ T + \text{GHSERPB}$
	(In)	298.14–2100	$+473.23 + 3.5531\ T + 2.14885 \times 10^{-05}\ T^2 - 0.0396834\ T \ln T + \text{GHSERPB}$
	β	298.14–2100	$+183.2 + 0.45314\ T + 2.14885 \times 10^{-05}\ T^2 - 0.0396831\ T \ln T + \text{GHSERPB}$
	L	298.14–600.63	$+4672.157 - 7.750257\ T - 6.0144 \times 10^{-19}\ T^7 + \text{GHSERPB}$
		600.63–5000	$+4853.112 - 8.066587\ T - 8.05644 \times 10^{25}\ T^{-9} + \text{GHSERPB}$
Sn	(Pb)	298.14–3800	$+4150 - 5.2\ T + \text{GHSERSN}$
	(Sn)	298.14–505.06	$-5855.135 + 65.427891\ T - 15.961\ T \text{Ln}T - 0.0188702\ T^2 + 3.121167 \times 10^{-6}\ T^3 - 61960\ T^{-1}$
		505.06–800	$+2524.724 + 3.989845\ T - 8.2590486\ T \ln T - 0.016814429\ T^2 + 2.623131 \times 10^{-6}\ T^3 - 1081244\ T^{-1} - 1.2307 \times 10^{25}\ T^{-9}$
		800–3000	$-8256.959 + 138.981456\ T - 28.4512\ T \ln T - 1.2307 \times 10^{25}\ T^{-9}$
	(In)	298.14–3800	$+5015.5 - 7.5\ T + \text{GHSERSN}$[a]
	β	298.14–3000	$+5015.5 - 7.5\ T + \text{GHSERSN}$[a]
	L	298.14–505.06	$+7104.222 - 14.09088\ T + 1.49316649 \times 10^{-18}\ T^7 + \text{GHSERSN}$
		505.06–3000	$+6970.705 - 13.813302\ T + 1.24912 \times 10^{26}\ T^{-9} + \text{GHSERSN}$

L: liquid.
[a] Taken from [8] whereas the others are taken from [1].

as ${}^0G_i^{\varphi}(T) - {}^0H_i^{\Phi}$ (298.15 K) where ${}^0G_i^{\varphi}(T)$ is the molar Gibbs energy of the pure element i in the physical state φ at temperature T and where ${}^0H_i^{\Phi}$ (298.15 K) is the molar enthalpy of the stable state of i at 298.15 K. These data are reported in Table 6. Table 7 gives the crystal structures of the different phases. The molar Gibbs energy of a phase φ, $G^{\varphi}(T)$, is expressed by:

$$G^{\varphi}(T) - \sum_i x_i H_i^0(298.15\,\text{K}) = G^{\varphi,\text{ref}} + G^{\varphi,\text{id}} + G^{\varphi,\text{ex}} \tag{1}$$

where x_i is the molar fraction of the element i in the φ-phase. In this optimization, the liquid phase, the two intermediate phases β and γ, and the three primary solid solutions (tetragonal (In), face-centered cubic (Pb) and body-centered tetragonal (βSn)) are described as disordered solutions. The molar Gibbs energy of mixing is expressed by the Redlich–Kister–Muggianu [5,6] model. In this case the different terms are expressed as:

$$G^{\varphi,\text{ref}} = \sum_i x_i({}^0G_i^{\varphi}(T) - {}^0H_i^{\Phi}(298.15\,\text{K})) \tag{2}$$

$$G^{\varphi,\text{id}} = RT\sum_i x_i \ln x_i \tag{3}$$

$$G^{\varphi,\text{ex}} = \sum_i \sum_{j\neq i} x_i x_j \sum_{\upsilon} L_{i,j}^{\upsilon,\varphi}(x_i - x_j)^{\upsilon} + x_i x_j x_k (L_{i,j,k}^{0,\varphi} x_i + L_{i,j,k}^{1,\varphi} x_j + L_{i,j,k}^{2,\varphi} x_k) \tag{4}$$

where the $L_{i,j}^{\upsilon,\varphi}$ parameters are dependent on the temperature.

$$L_{i,j}^{\upsilon,\varphi} = a_{i,j}^{\upsilon,\varphi} + b_{i,j}^{\upsilon,\varphi} T \tag{5}$$

Table 7
Crystal structure of the solid phases of the In–Pb and the In–Sn systems

Phase	Pearson symbol	Space group	Strukturbericht designation	Prototype
(In)	tI2	I4/mmm	A6	In
β	tI2	I4/mmm	A6	In
(Pb)	cF4	$Fm\bar{3}m$	A1	Cu
γ	hP5	$P6_3/mmm$		
(βSn)	tI4	$I4_1/amd$	A5	βSn
(αSn)	CF8	$Fd\bar{3}m$	A4	C (diamond)

4. Results and discussion

4.1. In–Pb

The optimization was performed using the Parrot module of Thermo-Calc [4] and the optimized parameters are presented in Table 8. Because of the lack of experiments for

Table 8
Set of parameters of the In–Pb–Sn system

Phase (disordered solution)	Parameter	Value (J mol^{-1} of atoms)
L	$L^{0,L}_{In,Pb}$	3679 − 1.0797 T
	$L^{1,L}_{In,Pb}$	605 − 1.3688 T
	$L^{0,L}_{In,Sn}$	−769 − 0.1312 T
	$L^{1,L}_{In,Sn}$	−119 − 0.3902 T
	$L^{0,L}_{Pb,Sn}$	+6200 − 0.418 T[a]
	$L^{1,L}_{Pb,Sn}$	+790 − 1.914 T[a]
	$L^{0,L}_{In,Pb,Sn}$	+515 − 8.7802 T
	$L^{1,L}_{In,Pb,Sn}$	−3881 + 19.9676 T
	$L^{2,L}_{In,Pb,Sn}$	+6550 − 30.8775 T
(In)	$L^{0,tet-a6}_{In,Pb}$	2390
	$L^{0,tet-a6}_{In,Sn}$	+578 − 1.1232 T
	$L^{1,tet-a6}_{In,Sn}$	−1156
	$L^{0,tet-a6}_{Pb,Sn}$	+6004
β	$L^{0,\beta}_{In,Pb}$	3645
	$L^{1,\beta}_{In,Pb}$	−533
	$L^{0,tet-\alpha}_{In,Sn}$	+774 − 5.4627 T
	$L^{1,tet-\alpha}_{In,Sn}$	−2379 + 4.5664 T
	$L^{1,tet-\alpha}_{Pb,Sn}$	+6000
(Pb)	$L^{0,fcc}_{In,Pb}$	3824
	$L^{1,fcc}_{In,Pb}$	603
	$L^{1,fcc}_{Pb,Sn}$	+7860 − 4.94 T[a]
	$L^{1,fcc}_{In,Pb,Sn}$	−4164 + 20 T
γ	${}^0G^{\gamma}_{In}$	+13448 − 19.6760 T
	${}^0G^{\gamma}_{Pb}$	+13098
	${}^0G^{\gamma}_{Sn}$	+700 − 1.3358 T
	$L^{0,\gamma}_{In,Sn}$	−17314 + 30.7559 T
	$L^{2,\gamma}_{In,Pb,Sn}$	−19677
(βSn)	$L^{0,bct}_{In,Sn}$	−2554 + 9.2776 T
	$L^{0,bct}_{Pb,Sn}$	+19700 − 15.89 T[a]

L: liquid.
[a] From [11].

solid alloys, we have chosen a regular solution model for the three solid solutions (In), β and (Pb) whereas the liquid phase is described with a subregular solution model.

Fig. 1 reveals the good agreement between the experimental data points and the calculated In–Pb phase diagram. Table 1 lists the calculated invariant equilibria and compares them with the data of Massalski [23]. Fig. 2 shows the calculated enthalpy of mixing of the liquid phase at 756 K drawn with reference to the pure liquid component in comparison with selected experimental results from [37–39]. We compare the activity measured by [32,33,35,36] to the calculated indium activity (referred to pure liquid In) at 673 and 973 K in Fig. 3(a), and the calculated lead activity at 673 and 1070 K (referred to pure liquid Pb) in Fig. 3(b). These values are correctly retranscribed.

4.2. In–Sn

The lattice stability of In and Sn in the γ-phase which are unavailable in the SGTE data bank had to be evaluated.

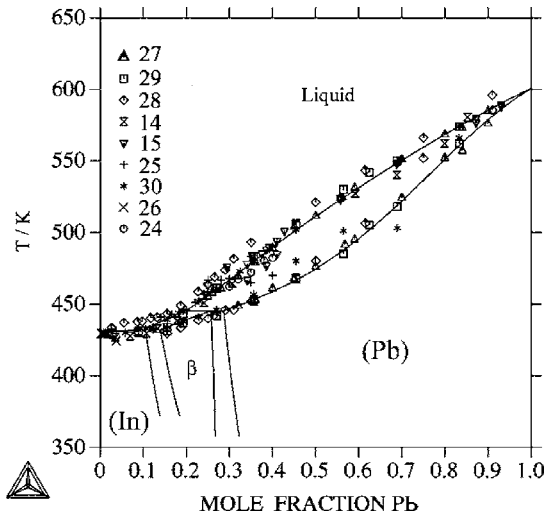

Fig. 1. Comparison of the calculated In–Pb diagram with experimental data.

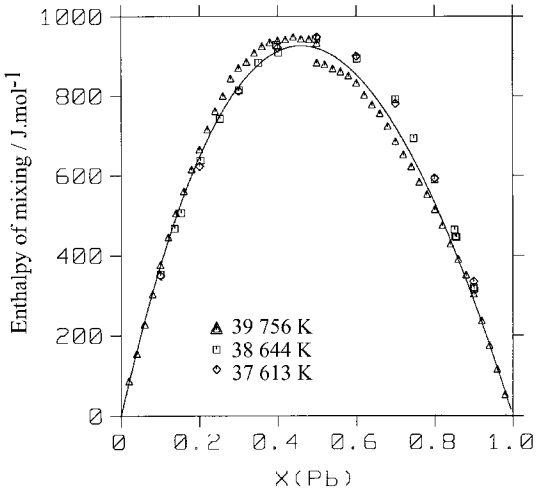

Fig. 2. Comparison between the calculated enthalpy of mixing of the liquid phase (solid line) of In–Pb at 756 K (referred to pure liquid) and experimental values (symbols) from [37–39].

The optimized parameters are presented in Table 8. The liquid, (In) and β-phases were described with a subregular solution model. The (βSn) and γ-phases were described with a regular solution model.

Fig. 4 shows the calculated In–Sn phase diagram obtained with the set of parameters taken from Table 8. The calculation is in agreement with the experimental values. However, the β/(β + γ) phase boundary from Wojtaszek and Kuzyk [47] is not reproduced because the phase diagram by Heumann and Alpaut [41]—which is well-accepted—offers a more tin-rich phase boundary. In Table 4 the calculated and experimental temperatures and compositions of invariant reactions taken from Massalski [23] are compared. All invariants agree well with an accuracy less than 1 at.% of tin. The maximum difference between the calculated and experimental temperatures of equilibrium is 1 K.

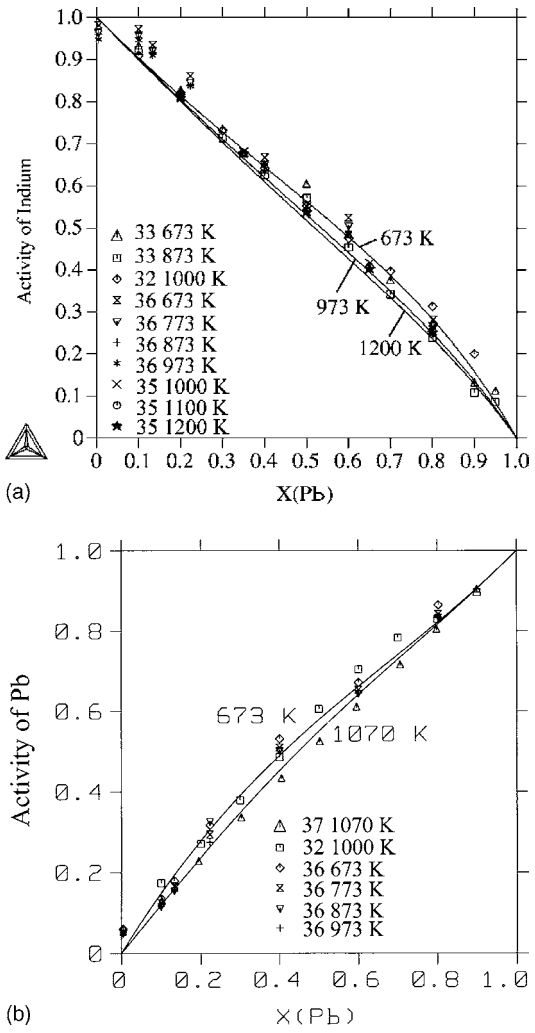

Fig. 3. (a) Calculated activity of indium for the liquid phase of In–Pb (solid line) calculated at 673, 973 and 1200 K (referred to the pure liquid indium) and comparison with experimental values (symbols) from [32,33,35,36]; (b) calculated activity of lead for the liquid phase of In–Pb (solid line) calculated at 673 and 1070 K (referred to pure liquid indium) and comparison with experimental values (symbols) from [31,32,36].

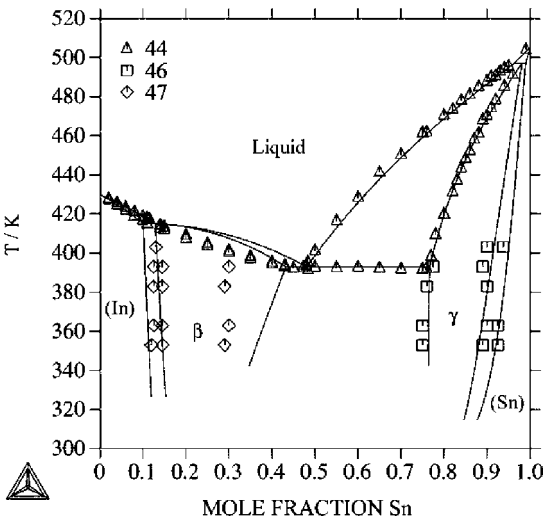

Fig. 4. Comparison of the calculated In–Sn diagram with experimental data.

Fig. 5(a) shows the comparison between the calculated enthalpy of mixing of the liquid phase at 673 K (referred to the pure liquid component) and experimental values from [38,48,49]. For the data of partial Gibbs energy of indium, two sets of experimental values, which cover the entire composition range, are available in literature [7,10]. These two authors give divergent results, so we only used the most recent data [7] in the optimization. On Fig. 5(b) we compare the calculated EMF versus temperature (from 630 to 830 K) with experimental values from Vassiliev et al. [7], for the same alloy compositions as these authors. There is an important gap between the restitution of the activities of In due to Terpilowski and Przezdziecka-Mycielska [10] and the calculation over the entire composition range. This is normal because we have preferred to be closer to Vassiliev information than those of Terpilowski and Przezdziecka-Mycielska.

In Fig. 5(c) the calculated enthalpy of mixing for solid phases at 373 K (referred to In(A6) and Sn(A5)) is compared with experimental values from [42,51]. We did not use the values of [42] in the calculation because they were derived from activity measurements and not from calorimetry contrary to these due to Alpaut and Heumann [51]. Fig. 5(d) shows a comparison between calculated activity of indium for the solid phases at 373 K (referred to the In(A6)) with experimental data from [42]. We note a good agreement in In-rich composition and an important deviation for Sn-rich alloys. These activity values of In in Sn-rich alloys are very difficult to reproduce by calculation without losing good agreement with the other experimental data. Some values of enthalpy of solidification measured by Alpaut and Heumann [51] were compared to these obtained by calculation and a good agreement over the entire composition range was obtained.

4.3. In–Pb–Sn

Considering the lack of data related to the solid phases, we have chosen to limit the number of parameters in the optimization of those phases. The γ-phase is not stable in the binary In–Pb system and not available in the SGTE data bank. It had to be evaluated. The liquid phase is described with three ternary coefficients. The optimized parameters are presented in Table 8.

Fig. 6(a) shows the calculated section joining the In–Pb binary and Pb–Sn binary near the two eutectic points in comparison with the results of Evans and Prince [13]. The calculated isoplethic cut at 2 wt.% In is presented on Fig. 6(b) and compared to [13]. The two invariant reactions are calculated with a discrepancy lower than 2 K: Liquid + (Sn) → (Pb) + γ at 445.7 K and Liquid + (Pb) → β + γ at 407.8 K. The liquidus curve falls in with the experimental points, but the solid phase boundaries are not well reproduced.

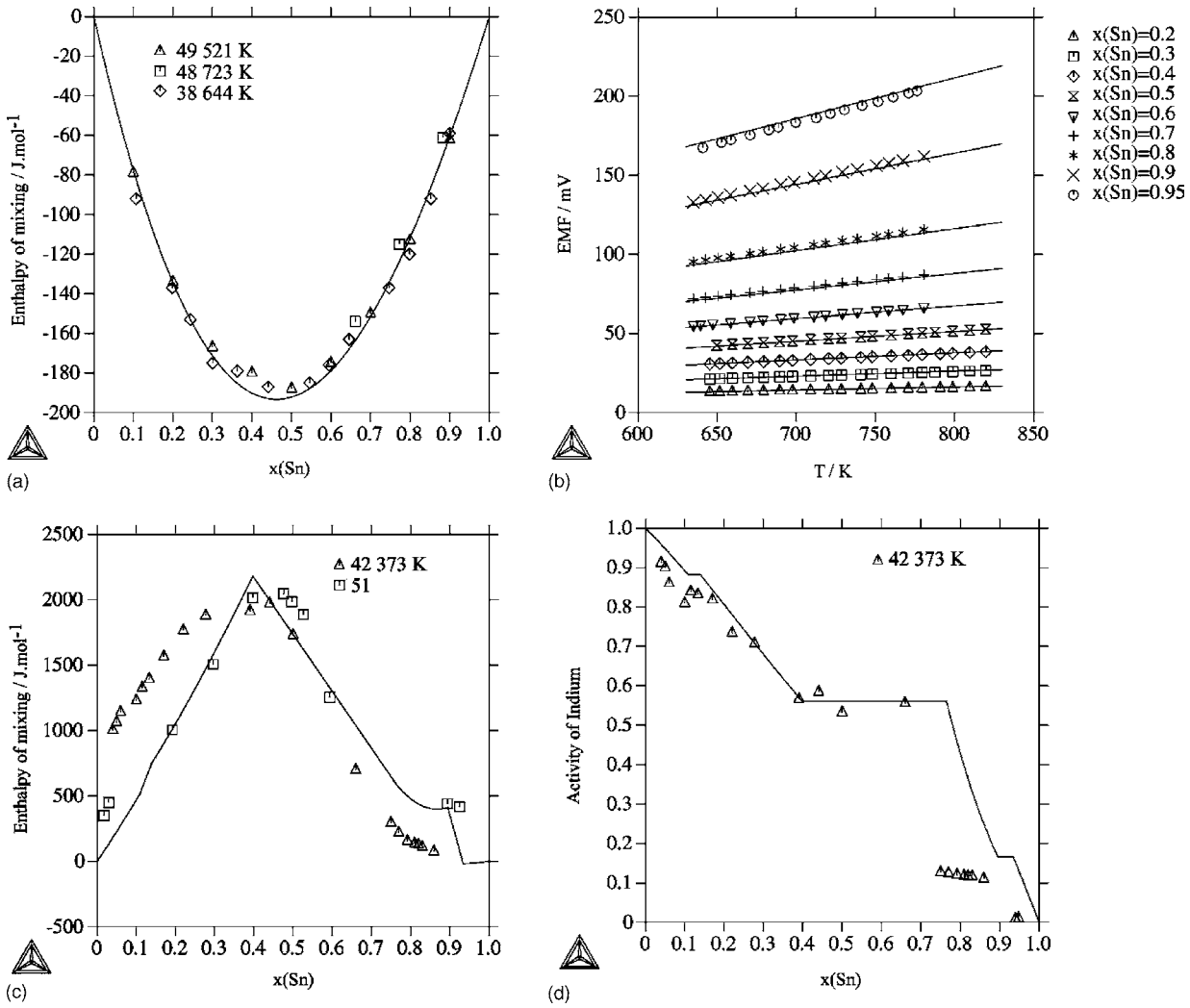

Fig. 5. (a) Comparison between the calculated enthalpy of mixing of the liquid phase (solid line) of In–Sn at 673 K (referred to the liquid phase) and experimental values (symbols) from [38,48,49]; (b) calculated electromotive forces (solid lines) between 630 and 830 K for nine alloys In_xSn_{1-x} (referred to the liquid phase) and comparison with experimental results (symbols) from [7]; (c) comparison between the calculated enthalpy of mixing for solid phases (solid line) of In–Sn at 373 K (referred to the In-tet-A6 and Sn-bct) and experimental values (symbols) from [42,51]; (d) calculated activity of indium for the solid phases of In–Sn (solid line) calculated at 373 K (referred to the In-tet-a6) and comparison with experimental data (symbols) from [42].

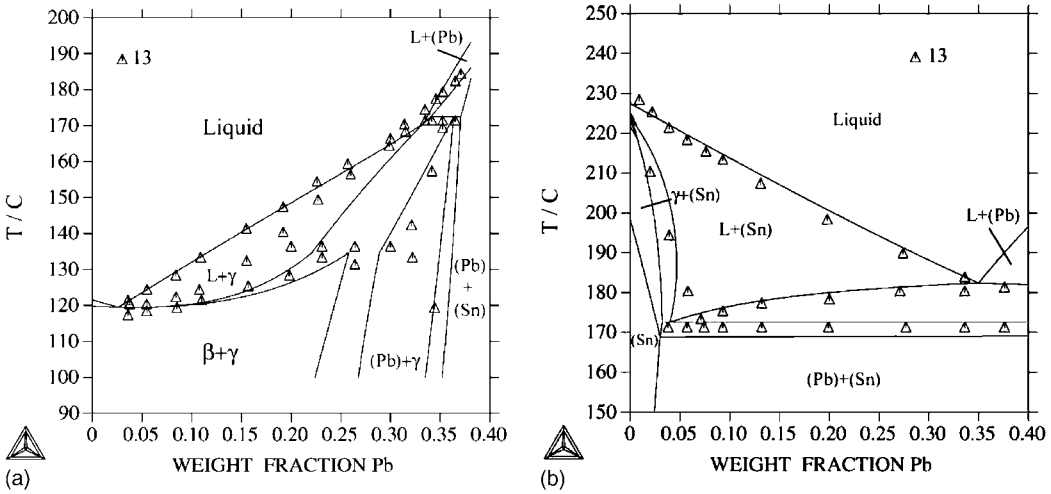

Fig. 6. (a) Comparison between the calculated section joining the In–Sn binary and the In–Pb binary near the two eutectic points and experimental values from [13]; (b) comparison between the calculated ternary section at 0.02 wt.% In and experimental values from [13].

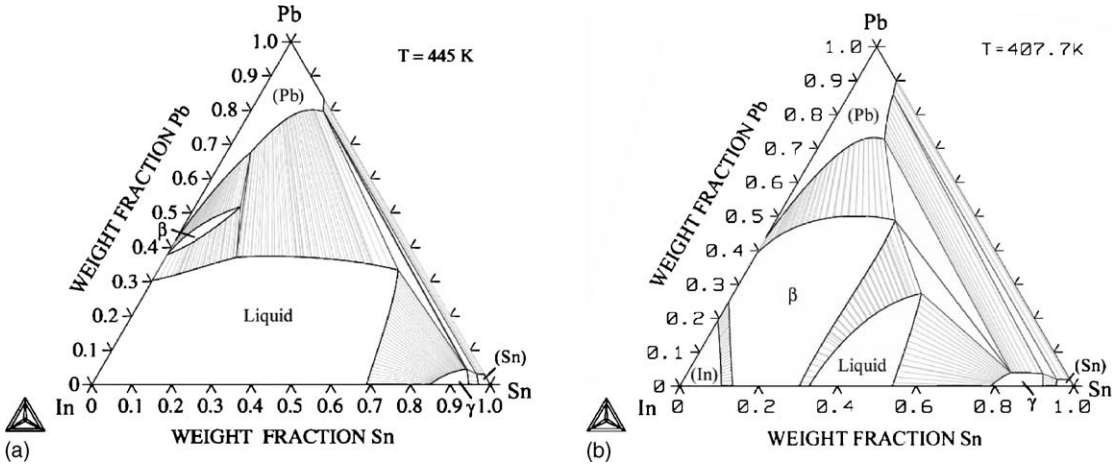

Fig. 7. (a) Calculated isothermal cut in ternary In–Pb–Sn system at 445 K; (b) calculated isothermal cut in ternary In–Pb–Sn system at 407.7 K.

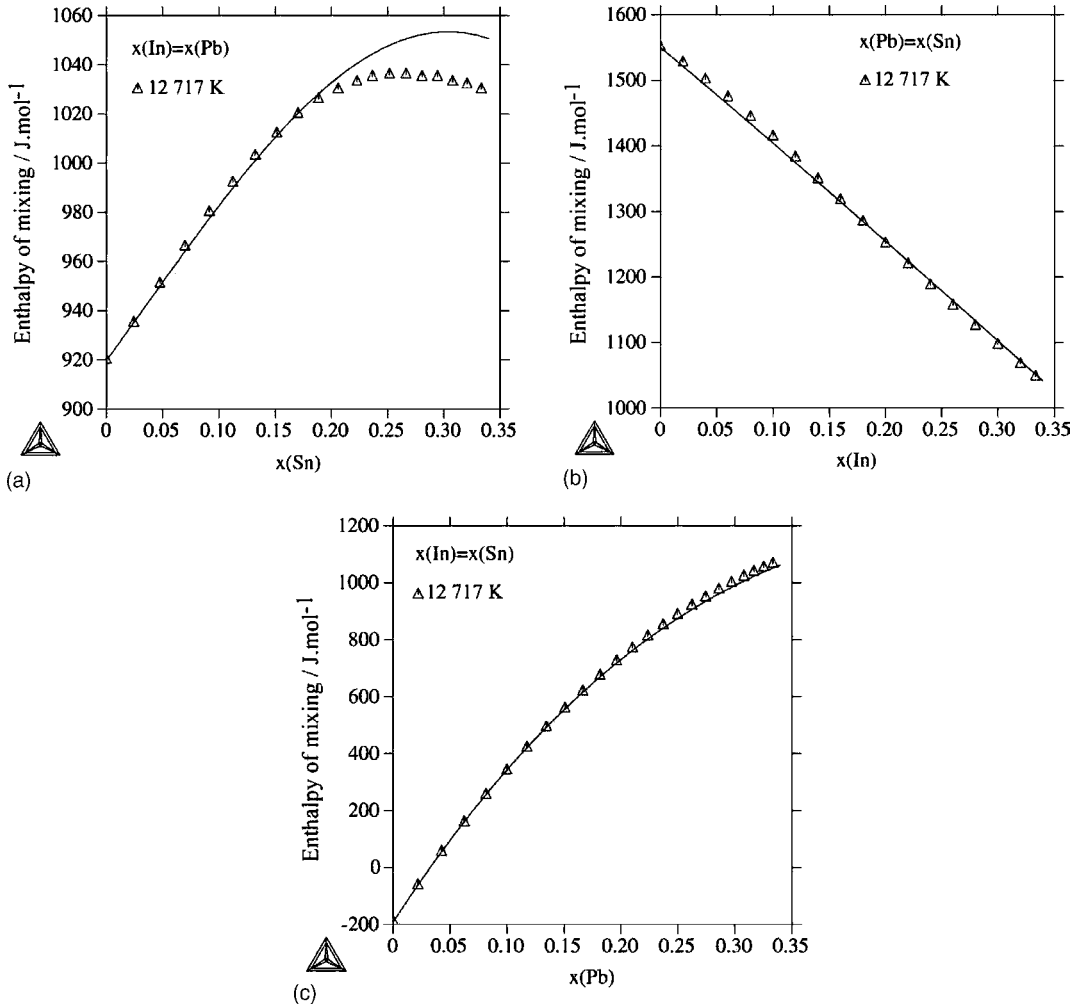

Fig. 8. (a) Comparison between the calculated enthalpy of mixing for liquid phase (solid line) at 717 K in the ternary In–Pb–Sn system (referred to the pure liquid components) following the isopletic cut $x_{In} = x_{Pb}$ and experimental values (symbols) from [12]; (b) comparison between the calculated enthalpy of mixing for liquid phase (solid line) at 717 K in the ternary In–Pb–Sn system (referred to the pure liquid components) following the isopletic cut $x_{Sn} = x_{Pb}$ and experimental values (symbols) from [12]; (c) comparison between the calculated enthalpy of mixing for liquid phase (solid line) at 717 K in the ternary In–Pb–Sn system (referred to the pure liquid components) following the isopletic cut $x_{In} = x_{Sn}$ and experimental values (symbols) from [12].

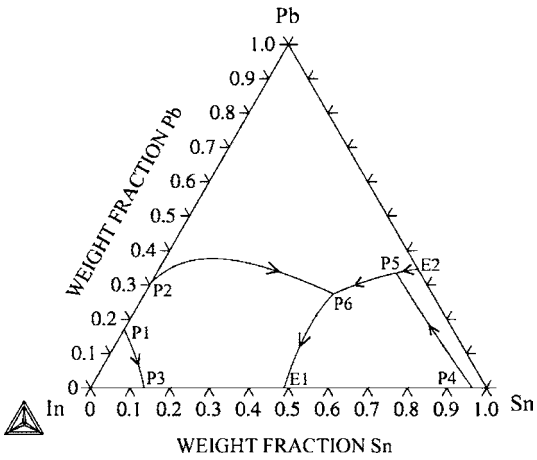

Fig. 9. Liquidus surface of In–Pb–Sn alloys.

Considering the few numbers of parameters used in this description, we have decided to respect the liquid-phase data and the invariant temperature reactions. The isothermal sections are calculated just below the two temperatures of the invariant reactions (Fig. 7(a) and (b)). Fig. 8(a–c) shows the comparison of the calculated enthalpy of mixing for the liquid phase at 717 K (referred to the pure liquid components) with experimental values from [12]: Fig. 8(a) follows the isopleticcut $x_{In} = x_{Pb}$, Fig. 8(b) follows the isopleticcut $x_{Sn} = x_{Pb}$, and Fig. 8(c) follows the isopleticcut $x_{In} = x_{Sn}$. There is a good agreement between experimental and calculated curves. The calculated liquidus surface is shown in Fig. 9. As suggested by Campbell et al. [26] no ternary eutectic is found in the ternary system. The monovariant curve descending from the In–Sn peritectic P4 meets the monovariant curve descending from the Pb–Sn eutectic E2, at the ternary point P5. The composition of the liquid phase at this point P5 is 6.1 wt.% In, 33.3 wt.% Pb and 60.6 wt.% Sn. The liquidus curve follows a line E2-P5 and meets then the monovariant curve descending from the In–Pb peritectic P2, at the ternary point P6. The composition of the liquid phase at this point P6 is 24.9 wt.% In, 27.6 wt.% Pb and 47.5 wt.% Sn. After P6, the liquidus curve ends at the binary In–Sn eutectic E1. In the In-rich corner, In–Pb peritectic P1 is linked with the In–Sn peritectic P3 as shown in Fig. 9.

5. Conclusions

A new thermodynamic assessment of the two systems In–Pb and In–Sn is carried out. A description of these systems is performed taking into account the more recent available thermodynamic and phase diagram data. Two consistent sets of adjustable parameters are obtained and are presented here. For the two systems, there is a good agreement between calculated thermodynamic functions and experimental values as well for liquid alloys as for solid alloys. A first thermodynamic description is proposed for the ternary In–Pb–Sn system. Isopleticcuts, isothermal sections just below the two temperatures of the ternary peritectic reactions and thermodynamic functions are calculated.

References

[1] A.T. Dinsdale, Calphad 15 (1991) 317.
[2] L. Kaufman, H. Bernstein, Computer Calculation of Phase Diagrams, Academic Press, New York, 1970.
[3] B. Sundman, B. Jansson, J.-O. Andersson, Calphad 9 (1985) 153.
[4] B. Jansson, Ph.D. Thesis, Royal Institute of Technology, Stockholm, 1984.
[5] O. Redlich, A.T. Kister, Ind. Eng. Chem. 40 (1948) 345.
[6] Y.M. Muggianu, M. Gambino, J.P. Bros, J. Chim. Phys. 72 (1975) 83.
[7] V. Vassiliev, Y. Feutelais, M. Sghaier, B. Legendre, Thermochim. Acta 315 (1998) 129.
[8] B.-J. Lee, C.-S. Oh, J.-H. Shim, J. Electron. Mater. 25 (1996) 983.
[9] T.-M. Korhonen, J.K. Kivilahti, J. Electron. Mater. 27 (1998) 149.
[10] J. Terpilowski, E. Przezdziecka-Mycielska, Archiwum Hutnictwa 5 (1960) 281.
[11] H. Ohtani, K. Okuda, K. Ishida, J. Phase Equilib. 16 (1995) 416.
[12] J.M. Fiorani, C. Naguet, J. Hertz, A. Bourkba, L. Bouirden, Z. Metallkd. 88 (1997) 711.
[13] D.S. Evans, A. Prince, Met. Sci. 14 (1980) 34.
[14] N.S. Kurnakow, N.A. Puschin, Z. Anorg. Allgem. Chem. 52 (1907) 430.
[15] S. Valentiner, A. Haberstroh, Z. Phys. B 110 (1938) 727.
[16] M. Hansen, K. Anderko, Constitution of Binary Alloys, McGraw-Hill, New York, 1958, p. 649.
[17] R. Hultgren, P.D. Desai, D.T. Hawkins, M. Gleiser, K.K. Kelley, Selected Values of Thermodynamic Properties of Binary Alloys, American Society for Metals, Metals Park, OH, 1973, p. 1283.
[18] J.P. Nabot, I. Ansara, Bull. Alloy Phase Diagr. 8 (1987) 246.
[19] C.R. Kao, J. Chin. Inst. Eng. 20 (1997) 315.
[20] A. Bolcavage, C.R. Kao, S.L. Chen, Y.A. Chang, in: P. Nash, B. Sundman (Eds.), Proceedings of the Symposium on Application of Thermodynamics in the Synthesis and Processing of Materials, TMS, Warrendale, PA, 1995, p. 171.
[21] D. Boa, I. Ansara, Thermochim. Acta 314 (1998) 79.
[22] D. Zivkovic, D. Minic, Z. Zivkovic, Tehnika 56 (2001) RGM1.
[23] T.B Massalski, Binary Alloy Phase Diagrams, American Society for Metals, Metals Park, OH, 1990.
[24] N. Ageew, V. Ageewa, J. Inst. Met. 59 (1934) 311.
[25] W. Klemm, H. Volk, Z. Anorg. Allgem. Chem. 256 (1947) 246.
[26] A.N. Campbell, R.M. Screaton, T.P. Schaefer, C.M. Hovey, Can. J. Chem. 33 (1955) 511.
[27] T. Heumann, B. Predel, Z. Metallkd. 57 (1966) 50.
[28] K.C. Liao, D.L. Johnson, R.C. Nelson, Mater. Res. Bull. 10 (1975) 1225.
[29] V.C. Marcotte, Scr. Metall. 12 (1978) 1.
[30] D.S. Evans, A. Prince, Met. Sci. 12 (1978) 600.
[31] D.H. Shiu, Z.A. Munir, High Temp. Sci. 3 (1971) 381.
[32] F. Sommer, Y.H. Suh, B. Predel, Z. Metallkd. 69 (1978) 470.
[33] J. Terpilowski, Z. Gregorezyk, Archiwum Hutnictwa 6 (1961) 197.
[34] K. Kameda, Y. Yoshida, S. Sakairi, Trans. Jpn. Inst. Met. 23 (1982) 433.
[35] M. Zheng, Z. Kozuka, J. Jpn. Inst. Met. 50 (1986) 804.
[36] D. Minic, D. Zivkovic, Z. Zivkovic, Thermochim. Acta 372 (2001) 85.
[37] E. Scheil, H.L. Lukas, Z. Metallkd. 52 (1961) 417.
[38] F.E. Wittig, P. Scheidt, Z. Phys. Chem. Neue Folge 28 (1961) 120.
[39] C. Naguet, J.M. Fiorani, A. Bourkba, J. Hertz, Z. Metallkd. 88 (1997) 469.
[40] H.I. Yoo, Ph.D. Thesis, University of California, Berkeley, CA, 1968.

[41] T. Heumann, O. Alpaut, J. Less-Common Met. 6 (1964) 108.
[42] O. Cakir, O. Alpaut, J. Less-Common Met. 141 (1988) 11.
[43] B. Predel, T. Gödecke, Z. Metallkd. 66 (1975) 654.
[44] D.S. Evans, A. Prince, in: L.H. Bennett, T.B. Massalski, B.C. Giessen (Eds.), Materials Research Society Symposium Proceeding 19, Elsevier North-Holland, 1983, p. 389.
[45] A.B. Kaplun, Teplofiz. Svoistva Rastvorov. 65 (1983).
[46] Z. Wojtaszek, H. Kuzyk, Zeszyty Naukowe Uniwersytetu Jagiellonskiego, Prace Chemiczne 19 (1974) 281.
[47] Z. Wojtaszek, H. Kuzyk, Zeszyty Naukowe Uniwersytetu Jagiellonskiego, Prace Chemiczne 21 (1976) 27.
[48] O.J. Kleppa, J. Phys. Chem. 60 (1956) 842.
[49] J.P. Bros, M. Laffitte, J. Chem. Thermodyn. 2 (1970) 151.
[50] A. Yazawa, T. Kawashima, K. Itagaki, J. Jpn. Inst. Met. 32 (1968) 1281.
[51] O. Alpaut, T. Heumann, Acta Metall. 13 (1965) 543.
[52] A.S. Skoropanov, E.I. Voronova, Termodinamicheskie Svoistva Metalicheskikh Splavov (1975) 249.